Correlating Fabrication Processes to the Microstructure and Deposition Properties of Mo Sputtering Targets

HUNG-SHANG HUANG, HUAN-CHIEN TUNG, CHUN-HAO CHIU and IN-TING HONG

New Materials Research & Development Department
China Steel Corporation

The way materials are processed influences the microstructure and consequently the properties of the materials. To better understand the relationship between process, microstructure and property for molybdenum used for sputtering, this study prepared molybdenum sputtering targets with different microstructures through using several metallurgical processes. The effects of the process and the microstructure on the sputtering properties of molybdenum were investigated. The results showed that a fully dense, fine-grained and randomly orientated molybdenum target exhibiting high deposition rate was obtained by hot isostatic pressing process. However, the electrical resistivity of the deposited molybdenum films was high due to the high oxygen content in the molybdenum target. Molybdenum only reached 97% density by hydrogen sintering. The density could reach 100% through the further rolling process, but the deposition rate obviously decreased after the plastic working. Although annealing treatment after rolling could change the microstructure from deformed to recrystallized and thus improve the deposition rate, the value was still lower than that of the sintering. This is possibly attributable to the intense decrease of (110) texture which exhibited the highest sputter yield for molybdenum. Theses results are helpful for us to develop a molybdenum target with a higher deposition rate for use in industry. By adjusting the process of target fabrication to control the grain size, lattice strain and texture, a significant improvement in the deposition rate could be achieved.

Keywords: Molybdenum sputtering target, Microstructure, Process, Deposition rate

1. INTRODUCTION

Molybdenum (Mo) is an important sputtering material to deposit Mo thin film as a diffusion barrier layer or an electrode layer, which is used in the liquid crystal display (LCD), touch panel and thin-film PV (photovoltaics) industries due to its unique properties such as a high melting point, high thermal and electrical conductivities, and a low thermal expansion similar to that of silicon and glass[1-4]. Since the market of these industries has grown continuously in recent years, the demand for Mo sputtering targets is also steadily increasing. In general, sputtering targets can be fabricated either by a molten route or by powder metallurgy (PM), and possibly followed by thermo-mechanical treatment. PM is currently a more prevalent starting process for the fabrication of Mo targets because of its high melting point.

For sputtering targets applied in thin-film coating, the film performance and sputtering properties mainly depend on the target's purity and microstructures (such as density, grain size, and grain orientation). For instance, Gehman et al.[5] developed an indium-tin oxide target (ITO) in 1992 and found that an ITO target with a metallic contamination of more than 100 ppm degrades the film resistivity of the ITO film. Lo et al.[6,7] explored the effect of density of W and W-Ti sputtering targets on abnormally particle generation on the thin films, and found that voids existing in the sputtering targets tend to act as particle sources during sputtering. Dunlop et al.[8] studied AlSiCu sputtering targets used in the semiconductor industry and suggested that the fine-grained and grain-oriented characteristics of a target provided a significant improvement in deposition uniformity. Moreover, Michaluk[9] studied the deposition properties of a Ta target and suggested that both grain size and grain orientation contributed to the sputtering behavior of Ta, but that the variation in sputter rate is more sensitive to changes in grain size than to changes in texture. Therefore, it is important to control the impurity and microstructure to obtain a sputtering target with good performance. However, to our knowledge, very little information is available for Mo targets. In addition, since the microstructure of metals is strongly determined by their metallurgical process, the fabrication process is also necessary to take into

consideration for the development of Mo targets.

In this study, Mo targets with different microstructures were obtained through different metallurgical processes and examined by direct current magnetron sputtering. The relationship between microstructure and process and their effects on the deposition properties of Mo target were investigated, particularly on deposition rate.

2. EXPERIMENTAL METHOD

Four metallurgical processes, including hot isostatic pressing (HIP), hydrogen sintering (HS), sintering + rolling (SR), and sintering + rolling + annealing (SRA), were used to fabricate Mo targets with different microstructures. Fine Mo powder with more than 99.95% purity was used as the raw material in this study. The characteristics of the powder are given in Table 1. For the HIP process, the Mo powders were added to a stainless steel can almost to the top, allowing sufficient space for an evacuation tube to be welded to the can side walls. The can could then be evacuated and sealed after the can had been filled with the Mo powders. The sealed can was then placed in an HIP furnace (QIH-21, Avure Autoclave System Inc., Ohio, USA) and heated at high temperature ($>1200^{o}$C) and high pressure (>150 MPa) simultaneously to obtain a nearly full-density Mo compact. For the HS process, the Mo powders were formed into rectangular bars by cold isostatic pressing (CIP) with a pressure of 220 MPa. The green density was about 68.5±1%. The densification was carried out at high temperature ($>1750^{o}$C) for several hours in hydrogen. For the SR process, the hydrogen sintered Mo compacts were subsequently heated at high temperature ($>1200^{o}$C) and straight rolled with specific rolling reduction ratios to obtain Mo plates. For the SRA process, the as-rolled Mo plates were further heated at different temperatures for annealing treatment.

The Mo compacts or plates prepared by the 4 different processes were cut, ground, and polished to form circular sputtering targets with a diameter of 152 mm and a thickness of 6 mm. The Mo targets were sputtered to deposit Mo films on cover glasses by a magnetron sputtering system at a direct current power of 500 W and an Ar partial pressure of 2~10 torr. An alpha stepper (AS-IQ, KLA-Tencor Corp., California, USA) was used to measure the thickness of the Mo films in order to determine the deposition rate on the Mo targets. The resistivity of the Mo films was determined by the four-point probe method. To evaluate the effects of the target properties on the sputtering properties, a carbon/sulfur analyzer (EMIA-820V, HORIBA Ltd., Kyoto, Japan) and an oxygen/nitrogen analyzer (EMIA-620W, HORIBA Ltd., Kyoto, Japan) were employed to measure the C, N, S and O content in the Mo targets. The density of the Mo targets was measured by the Archimedes' method. The microstructure of the Mo targets was observed using an optical microscope (OM, DMRM, Leica Microsystems Inc., Wetzlar, Germany). The grain size was measured by the line-intercept method from metallographs taken by the OM. The hardness was measured by a Rockwell hardness tester (ATK-600, Mitutoyo Corp., Kawasaki, Japan). The reported density, grain size, and hardness data are an average of at least five measurements. In addition, an X-ray diffractometer (XRD, D8 ADVANCE, Bruker AXS Inc., Karlsruhe, Germany) with Mo Kα radiation was also employed to examine the grain orientations of the Mo targets for different fabrication processes.

3. RESULTS AND DISCUSSION

3.1 Comparison of microstructure and deposition properties

Figures 1(a) through 1(f) show the microstructure of the Mo targets fabricated by HIP, HS, SR and SRA. The annealing temperatures of the various SRA processes were 1000, 1150 and 1300°C, respectively. Table 2 compares the sintered density, grain size, hardness,

Table 1   Characteristics of the Mo powders used in this study

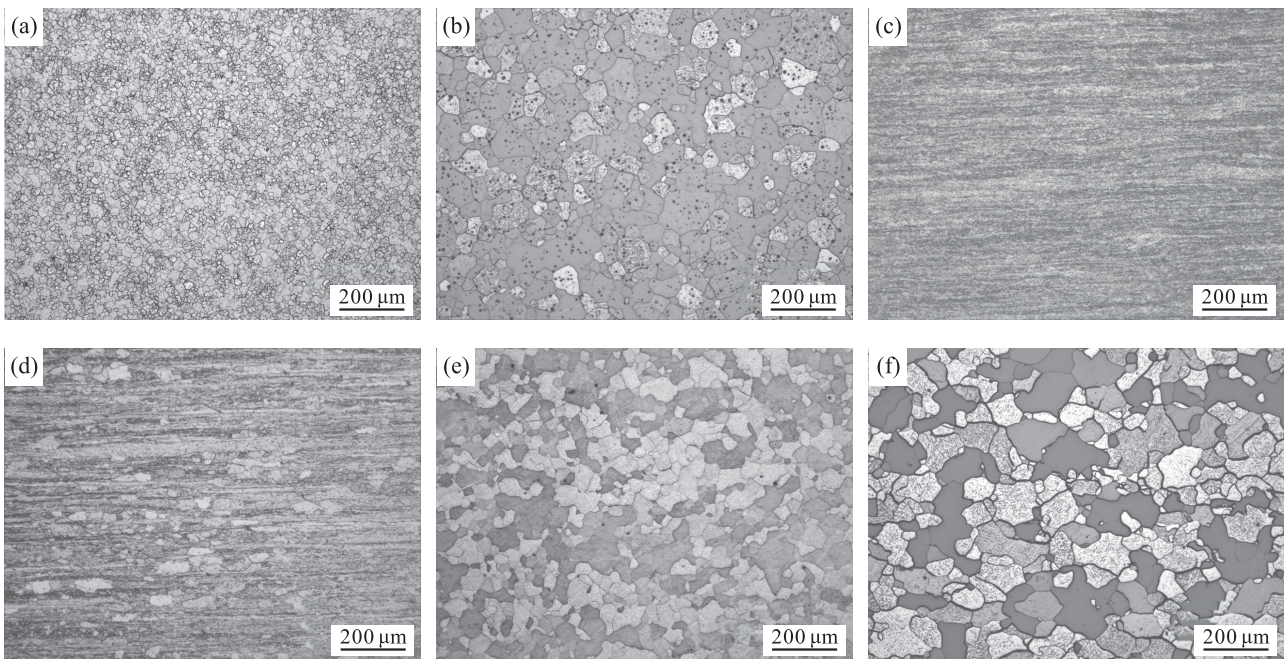| Characteristics	Mo powder
Manufacturing process	Gas reduced
Particle size (Fisher subsieve sizer)	3.1 μm
Shape	Polygonal aggregates
Arnold density	1.06 g/cm^3
Tapping density	3.01 g/cm^3
Chemistry	
C, wt%	0.004
S, wt%	0.001
N, wt%	0.005
O, wt%	0.160

Fig.1. Microstructures of Mo targets fabricated by different processes. (a) HIP, (b) HS, (c) SR, (d) SRA1000°C, (e) SRA1150°C, (f) SRA1300°C.

Table 2 Comparison of the target properties of Mo targets fabricated by different processes

Process	HIP	HS	SR	SRA1000°C	SRA1150°C	SRA1300°C
Target density (%)	99.9	97.0	100	100	100	100
Grain size (μm)	10.6	33.2	-	-	28.5	50.8
Hardness (HRB)	91.6	78.3	97.6	92.0	84.9	83.5
Impurity (ppm)						
C content	54	39	33	24	31	28
O content	890	52	72	62	82	74

and the carbon and oxygen content of the six Mo targets. It is illustrated that HIP process could fabricate a Mo target with nearly full density, so that there were almost no pores observed in Fig.1(a). In contrast, the density of Mo only reached 97% by hydrogen sintering, thus there were a few pores in Mo grains, as shown in Fig.1(b). Moreover, since the HIP temperature is quite low, the occurrence of grain growth was not obvious after the densification. Thus, the microstructure of the HIPed Mo was very fine. The average grain size only reached 11 μm, about 3 times smaller than that of the hydrogen sintered Mo. However, Table 2 shows that the oxygen content of the HIPed Mo was 890 ppm, much higher than that of the hydrogen sintered Mo. This is because Mo powder inherently exhibits surface oxide because of the reactivity of molybdenum with oxygen[10], so that the original oxygen content in Mo powders was quite high, at a level of 0.16 wt%. However, there is no hydrogen to effectively reduce the surface oxides of Mo powders during the HIP process.

Regarding the effect of target density on sputtering, Lo et al.[7] have reported that local voids within a target are the source of abnormal arcing. Arcing is characterized by the intense, localized concentrations of plasma supported by the collective emission of electrons from the target surface[11]. The occurrence of unstable arcs at void sites facilitates the easy formation of nodules around the voids and thus leads to explosive ejection of damaging macro-particles during sputtering. Since the hydrogen sintering process in this study had difficulty in attaining full density for Mo, such a Mo target with some voids might also be harmful to sputtering.

For improvement in the target density of the

sintered Mo, Figure 1(c) shows that the sintering pores could be eliminated by the SR process. The density of Mo checked by the Archimedes' method reached 100% after plastic rolling. However, the Mo grains become elongated along the rolling direction to form a fiber structure. For the various SRA processes, the variations in microstructure, hardness and grain size with annealing temperature demonstrate that when the annealing temperature was at 1000°C, a few new grains appeared and the hardness decreased from HRB 97.6 to HRB 92, indicating the occurrence of recrystallization. A fully recrystallized microstructure was achieved at 1150°C and the hardness further decreased to HRB 85. As the annealing temperature further increased to 1300°C, the phenomenon of grain growth occurred and the grain size increased from 28.5 to 50.8 μm.

To understand whether the differences in microstructure and impurity among these fabrication processes influence the deposition properties for the Mo sputtering target, the six Mo targets were sputtered under several sputtering conditions for comparison. Figure 2 compares the deposition rate of the six targets. The HIPed Mo exhibited the highest deposition rate, followed by the hydrogen sintered Mo, while the as-rolled Mo showed the lowest rate. The average deposition rates of the three targets were 24.0, 23.0 and 20.6 Å/sec, respectively, indicating the last one is much slower than the two former ones. However, the deposition rate of the as-rolled Mo could be significantly improved by a further appropriate amount of annealing. The deposition rate only slightly increased when the as-rolled Mo was annealed at 1000°C, while the deposition rate significantly increased to a maximum value at 1150°C. As the temperature further increased to 1300°C, the deposition rate declined again. Nevertheless, the maximum deposition rate of the annealed as-rolled
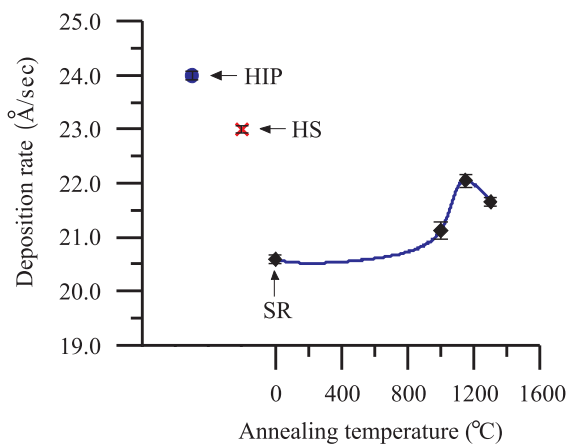
Mo remained lower compared to the HIPed Mo and the hydrogen sintered Mo. In addition, although the Mo target fabricated by the HIP process exhibited the highest deposition rate, the electrical resistivity of Mo film shown in Fig.3 indicates that all Mo thin films sputtered by the HIPed Mo target exhibited higher resistance. This could be very likely attributed to the higher oxygen content in the HIPed Mo target as shown in Table 2. Thus, to improve the conductivity of Mo thin-film sputtered by the HIPed Mo target, a pretreatment of Mo powders to decrease the oxygen content before the HIPing process is necessary.
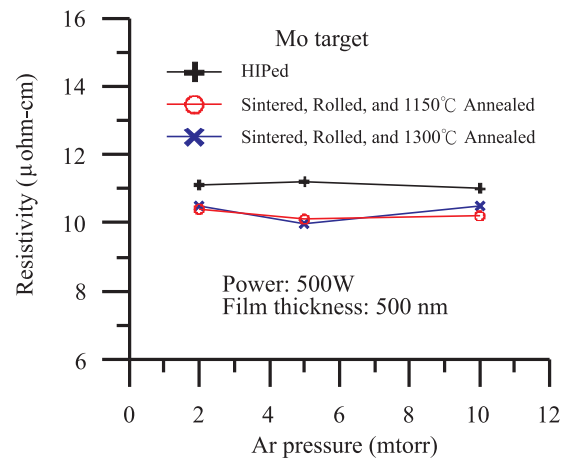

Fig.3. Comparison of the film resisitvity of Mo targets sputtered at different Ar pressures for the HIPed Mo, the 85% rolled + 1150°C annealed Mo, and the 85% rolled + 1300°C annealed Mo.

3.2 Discussion of the relationship between microstructure and deposition rate of Mo target

We think the main cause of the higher deposition rate of the HIPed Mo compared to the sintered Mo is that the HIPed Mo possessed a very fine-grained microstructure, which has a higher volume fraction of grain boundaries. Since atoms located at the grain boundaries are arranged disorderly from the original lattice sites, grain boundary areas are defects in the crystal structure. It is believed that the high interfacial energy and relatively weaker bonding of grain boundaries makes them the easier sites for bombardment and ejection of atoms during sputtering. As a result, the fine-grained HIPed Mo target exhibited a higher deposition rate. Moreover, the cause of the much slower deposition rate of the as-rolled Mo should be related to the heavy distortion of the Mo crystal lattice caused by the process of plastic deformation. This is because, as illustrated in Fig.4[12], the sputtering process theoretically starts at the penetration of an energetic plasma ion

Fig.2. Comparison of the deposition rate of Mo targets fabricated by HIP, HS, SR and SRA processes.

into a solid target. The ion passes through several subsurface layers of atoms and collides with an inner atom of the target. Adequate energy of the ion is transferred to the atom and dislodges it from the original position. The dislodged atom then transfers its momentum to the adjacent atoms successively through subsequent collision cascades[13]. If sufficient momentum is eventually transferred to a surface atom and remains higher than the surface binding energy, the surface atom will be ejected. Since the crystal lattice of the as-rolled Mo was heavily distorted, it might be detrimental to the conducting of collision cascade. This indicates that the final kinetic energy of surface atoms derived from the collision cascade might be affected, eventually leading to low deposition rate. Therefore, as the working strain stored in the as-rolled Mo was eliminated through the recrystallization treatment at 1150°C, the deposition rate was significantly improved from 20.6 to 21.1 Å/sec, proving the argument that the interference of collision cascade arises from the distortion of Mo lattice is reasonable.
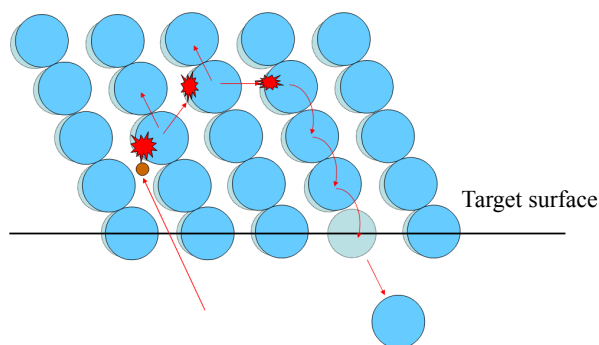

Fig.4. Schematic illustration of sputtering process in a crystalline sputtering target [12].

Although Figure 2 showed that the deposition rate of as-rolled Mo could be obviously improved through the annealing treatment at 1150°C, the value was still lower compared to the originally sintered Mo target. Since the average grain size of the 1150°C annealed Mo was 28.5 μm, even a little smaller compared to that of the sintered Mo, the decrease in deposition rate of the SRA Mo must be attributed to other factors, rather than grain boundary and lattice distortion. Previous literature has reported that grain orientation is also an important factor to affect the deposition rate and deposition uniformity of sputtering targets[8,9]. To understand the grain orientation of target surface of Mo, the Mo targets fabricated by the different processes were examined by X-ray diffraction. Figure 5 demonstrates that both XRD patterns of the HIPed Mo and the sintered Mo were very similar to that of Mo powders, indicating the random distribution of grain orientation

for the two Mo targets. However, as the sintered Mo was rolled, the XRD pattern changed. The peak intensity of (110) plane decreased obviously while the peak of (100) plane increased significantly. When the as-rolled Mo was further annealed, the XRD pattern showed an intense preferred orientation of (100) planes aligned along the target surface. These results suggest that it is detrimental to the deposition rate when the texture of Mo target is transformed from random to intensely (100) orientated.
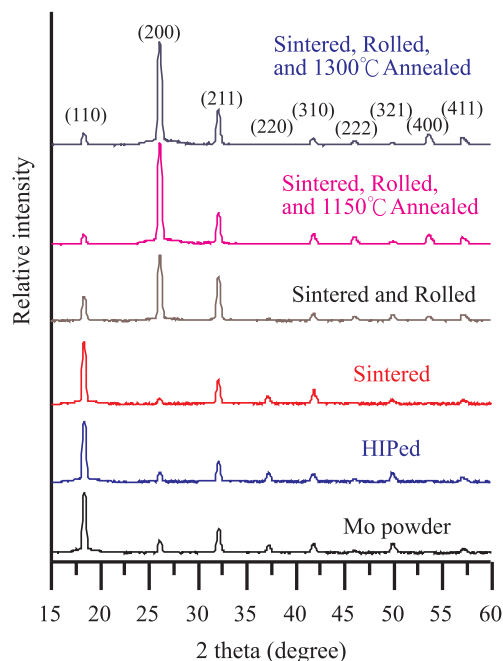

Fig.5. X-ray diffraction patterns of Mo powder and the Mo targets fabricated by different processes.

It is known that the sputter yield (Y), which is defined as the average number of atoms removed from the sputtering target per incident ion, depends not only on the target material and ion, but also on the crystal orientation of the target[14]. Previous literature has mainly prepared monocrystalline targets in various low-index crystallographic planes for sputtering work in order to understand the effect of crystal orientation. For instance, Magnuson and Carlston[15] explored the sputtering yields of Cu and Ag single crystals for the three main low-index planes in 1963, and found that (111) plane exhibits the highest sputter yield, followed by (100) plane, with (110) plane showing the lowest yield. Moreover, Robinson and Southern[16] reported in 1967 the same sputtering results for Au and Al single crystals, namely, $Y_{(111)} > Y_{(100)} > Y_{(110)}$ for face centered cubic (fcc) metals. However, little information has been provided on body centered cubic (bcc) refractory metals by experimental results, probably due to more

difficult preparation of those single crystal targets in the past. To know which of the three low-index planes exhibits the highest or lowest sputter yield for bcc Mo, a method without using single crystal targets was introduced in this study through using the techniques of electron backscattered diffraction (EBSD), focused ion beam (FIB), and atomic force microscope (AFM). A schematic procedure of this method is shown in Fig.6.
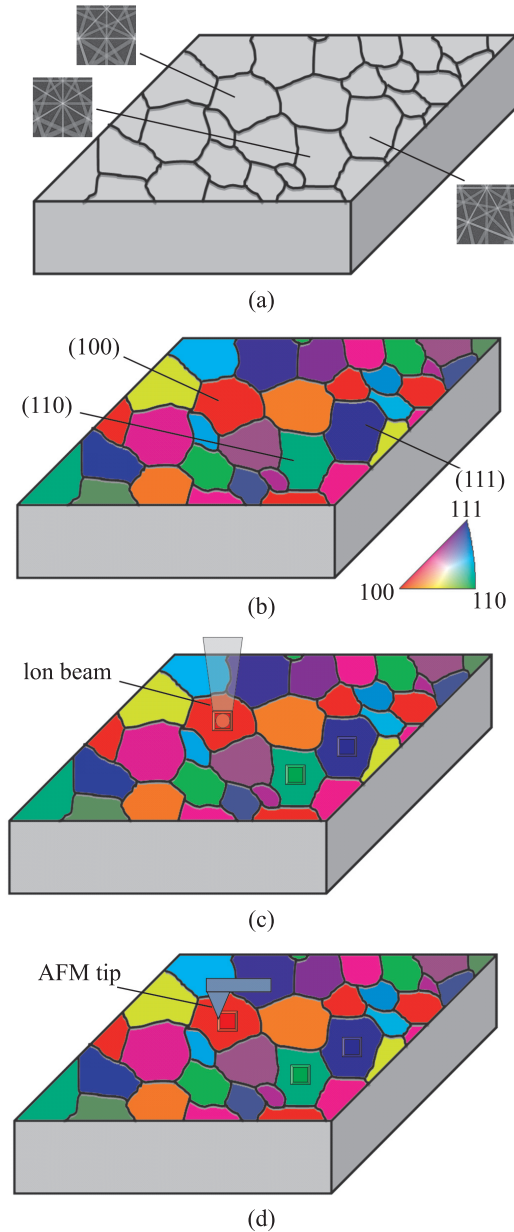

(a)

(b)

(c)

(d)

Fig.6. Schematics of the procedure for determining the sputter yields of low-index crystalline orientations of Mo: (a) a polycrystalline Mo sample with different grain orientations; (b) orientation identification by EBSD; (c) micro-sputtering by FIB; and (d) measurement of milled volume by AFM.

Firstly, an EBSD was employed to identify the crystal orientation for individual grains of a polycrystalline Mo specimen, so that the positions of grains with exactly (100), (110) and (111) planes could be located individually. Then, an FIB was used to perform the micro-milling to form a pattern of square shaped holes on these identified low-index grains. Next, an AFM was used to accurately measure the depth of erosion for each grain. Finally, the sputtering yield of different crystalline planes $Y_{(uvw)}$ for Mo could be calculated from the FIB experiment by the following formula:

$$Y_{(uvw)} = \frac{N_{target}}{N_{ion}} = \frac{\dfrac{N_A \cdot V \cdot \rho}{m_{target}}}{\dfrac{i \cdot t}{e}} = \frac{e \cdot N_A \cdot A \cdot h_{(uvw)} \cdot \rho}{m_{target} \cdot i \cdot t}$$

Where e is the elementary charge (1.6×10^{-19}), N_A is the Avogadro constant (6.02×10^{23}), A is the erosion area, $h_{(uvw)}$ is the erosion depth of a Mo crystalline plane (uvw), ρ is the Mo target density, m_{target} is the Mo molecular weight, i is the ion beam current, and t is the sputtering time.

The measured sputter yield, shown in Fig.7, evidently demonstrates that (110) plane exhibited the highest sputter yield, followed by (100) plane, while (111) plane showed the lowest yield for Mo. The trend was consistent with the rankings of the theoretical calculation of their planar packing fraction shown in Fig.8, indicating the intense correlation between the sputter yield and the planer packing fraction. Based on the sputtering process shown in Fig.4, it is believed that the transparency of ion in those different planes was not consistent. This indicates that when an accelerating ion vertically penetrated a crystalline plane with a higher planar packing fraction, such as Mo (110) plane, the ion merely penetrated a few subsurface layers and then immediately collided with atoms for momentum transfer, namely the occurrence of the collision cascade at a shallower layer. On the contrary, a lower planar packing plane such as Mo (111) could be penetrated deeply by an ion with the same energy, with the collision cascade thus occurring at a deeper layer. Therefore, different crystalline planes of Mo affected the penetrating depth of ions, and further affected the final kinetic energy of surface atoms derived from the collision cascade, eventually leading to a different sputter yield. That is to say, the low transparency of Mo (110) plane implied a shallower penetration, resulting in a higher sputtering yield. Accordingly, the extremely small number of (110) grains in the target surface of the annealed Mo is believed to be responsible for its lower deposition rate compared to the sintered Mo.
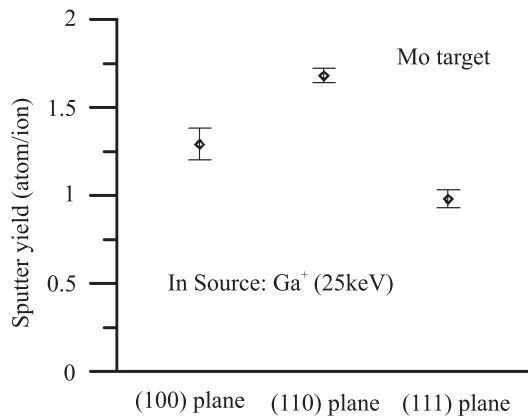
Fig.7. Comparison of the measured sputter yields for (100), (110) and (111) plane of Mo after FIB micro-milling.
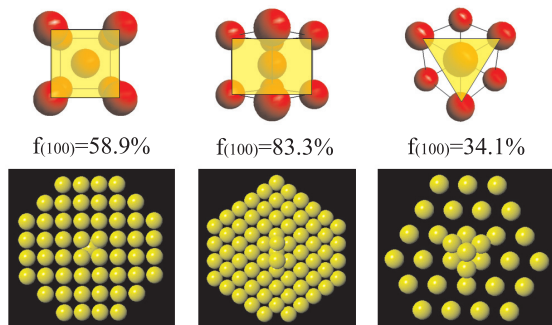

f(100)=58.9%   f(100)=83.3%   f(100)=34.1%

Fig.8. Sketch of the planar packing arrangement of atoms at the three low-index planes in bcc structure.

Based on the above experimental results, the factors that affect the deposition rate of a sputtering target during the sputtering process can be divided into three stages. Each stage and its meaning of physical metallurgy for materials can be described as follows. The first stage is the transparent depth of the incident ion, while the corresponding meaning is the texture intensity of the target surface. More (111) grains for fcc or more (110) grains for bcc aligned along the target surface is preferable for obtaining a high deposition rate. The second stage is the difficulty of the occurrence of a collision cascade, while the corresponding meaning is the degree of the lattice distortion. A target with a heavy plastic deformation is detrimental to its deposition rate. The third stage is the difficulty of the ejection of the surface atoms, namely the surface binding energy. A target with a smaller grain size exhibits more and weaker bonding atoms at its grain boundaries and thus is favorable for deposition rate. Such findings are very useful for us to develop Mo targets, because some control of texture, lattice strain, and grain size is possible by the proper choice of production processes

or variables in order to obtain a Mo target with a higher deposition rate. For instance, Figure 9 shows the comparison of the two Mo targets fabricated by straight rolling and cross rolling, respectively, at the same reduction rate, and further by annealing at the same temperature. Apparently, the texture intensity with (110) planes parallel to the target surface was significantly improved as the rolling process was changed from straight to cross. As a result, the deposition rate of the Mo target was also significantly improved.
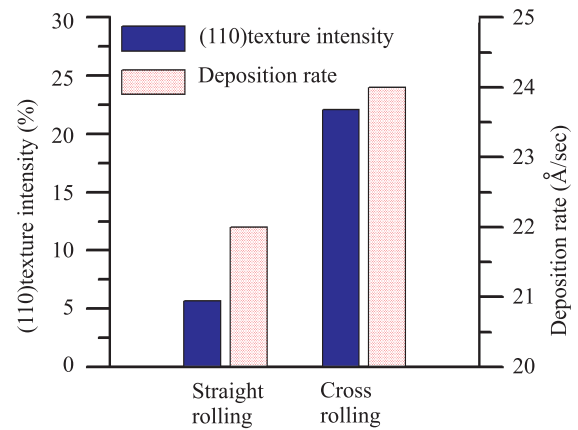

Fig.9. The (110) texture intensity and deposition rate of Mo sputtering targets fabricated by straight rolling and cross rolling.

4. CONCLUSIONS

The correlation between the fabrication process, the microstructure, and the texture, and their effects on the performance of the Mo sputtering target were investigated. It was concluded that HIP process could obtain a Mo target with fully density, fine grain microstructure and random crystal orientation. The target exhibited the highest deposition rate in this study. Conventional hydrogen sintering process could not obtain a Mo target with fully density. Although the sintering pores could be eliminated by plastic rolling, the deposition rate of the rolled Mo target was significantly decreased, due to the interference of occurrence of collision cascades by heavy lattice distortion during sputtering. The deposition rate of the rolled Mo could be improved through a suitable recrystallization treatment. However, the deposition rate of the annealed Mo was not as good as that of the sintered Mo. Since the micro sputtering of the three low-index crystal planes of Mo by FIB demonstrated that (110) plane exhibited the highest sputter yield, the intense decrease of (110) grains aligned along the target surface of the Mo target fabricated by the sintering + rolling + annealing process is very likely to be the cause of the lower deposition

rate. Based on these results, the factors that affect the deposition rate for Mo sputtering target include grain size, lattice distortion and grain orientation. By adjusting the fabricating process to control these factors, significant improvement in the deposition rate of a Mo target could be achieved.

<div align="center">

REFERENCES

</div>

1. H. Walser and J. A. Shields: IMOA (International Molybdenum Association) Newsletter, July 2007.
2. N. Kinsman and C. Kovach: IMOA MolyReview, January 2010, pp. 4-5.
3. G. Barrett and R. Omote: Inf. Disp, 2010, vol. 26, pp. 16-21.
4. K. Orgassa, H. W. Schock and J. H. Werner: Thin Solid Films, 2003, vols. 431-432, pp. 387-91.
5. B. L. Gehman, S. Jonsson, T. Rudolph, M. Scherer, M. Weigert and R. Werner: Thin Solid Films, 1992, vol. 220, pp. 333-6.
6. C. F. Lo, D. McDonald, D. Draper and P. Gilman: J. Electron. Mater., 2005, vol. 34, pp. 1468-73.
7. C. F. Lo and P. Gilman: J. Vac. Sci. Technol. A, 1999, vol. 17, pp. 608-10.
8. J. A. Dunlop, B. Y. Pouliquen, T. J. Drinnon, D. T. Wilcoxen, J. C. Huneke, I. C. Ivanov, D. B. Knorr and D. P. Tracy: J. Vac. Sci. Technol. A, 1993, vol. 11, pp. 1558-65.
9. C. A. Michaluk: J. Electron. Mater., 2002, vol. 31, pp. 2-9.
10. H. S. Huang and K. S. Hwang: Metall. Mater. Trans. A, 2002, vol. 33, pp. 657-64.
11. A. Anders: Thin Solid Films, 2006, vol. 502, pp. 22-8.
12. C. A. Michaluk: "Metallurgical Factors Affecting the Performance of Tantalum Sputtering Targets", pp. 75-81 in Proc. 41th Int. Symp. on Tantalum and Niobium, Brussels, Belgium, 2000.
13. R. S. Averback and T. D. Rubia: Solid State Phys., 1997; vol. 51, pp. 281-402.
14. R. Behrishch: Sputtering by Particle Bombardment I: Physical Sputtering of Single-Element Solids, Springer-Verlag, Berlin, 1981, pp. 219-60.
15. G. D. Magnuson and C. E. Carlston: J Appl Phys., 1963, vol. 34, pp. 3267-73.
16. M. T. Robinson and A. L. Southern: J Appl Phys., 1967, vol. 38, pp. 2969-73. □